Journal of Crystal Growth 312 (2010) 3574–3578

Contents lists available at ScienceDirect

Journal of Crystal Growth

journal homepage: www.elsevier.com/locate/jcrysgro

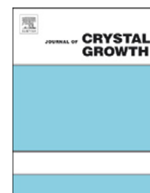

Method for modulating the wafer bow of free-standing GaN substrates via inductively coupled plasma etching

Kuei-Ming Chen [a,b,*], Yen-Hsien Yeh [a], Yin-Hao Wu [a], Chen-Hao Chiang [a], Din-Ru Yang [a], Chu-Li Chao [a,b], Tung-Wei Chi [b], Yen-Hsang Fang [b], Jenq-Dar Tsay [b], Wei-I Lee [a]

[a] Department of Electrophysics, National Chiao Tung University, 1001 University Road, Hsinchu 30010, Taiwan
[b] Electronics and Optoelectronics Research Laboratories, Industrial Technology Research Institute, Hsinchu, Taiwan

ARTICLE INFO

Article history:
Received 26 May 2010
Received in revised form
31 August 2010
Accepted 16 September 2010
Communicated by M. Schieber
Available online 24 September 2010

Keywords:
A1. Etching
A1. GaN substrate
A3. Hydride vapor phase epitaxy
B1. Nitrides
B2. GaN

ABSTRACT

The bowing curvature of the free-standing GaN substrate significantly decreased almost linearly from 0.67 to 0.056 m^{-1} (i.e. the bowing radius increased from 1.5 to 17.8 m) with increase in inductively coupled plasma (ICP) etching time at the N-polar face, and eventually changed the bowing direction from convex to concave. Furthermore, the influences of the bowing curvature on the measured full width at half maximum (FWHM) of high-resolution X-ray diffraction (HRXRD) in (0 0 2) reflection were also deduced, which reduced from 176.8 to 88.8 arcsec with increase in ICP etching time. Decrease in the nonhomogeneous distribution of threading dislocations and point defects as well as V_{Ga}–O_N complex defects on removing the GaN layer from N-polar face, which removed large amount of defects, was one of the reasons that improved the bowing of the free-standing GaN substrate. Another reason was the high aspect ratio of needle-like GaN that appeared at the N-polar face after ICP etching, which released the compressive strain of the free-standing GaN substrate. By doing so, crack-free and extremely flat free-standing GaN substrates with a bowing radius of 17.8 m could be obtained.

© 2010 Elsevier B.V. All rights reserved.

1. Introduction

Currently, III-nitride devices are grown on different substrates, such as GaN, sapphire, Si, and SiC substrates. The performance of III-nitride devices grown on sapphire, Si, and SiC substrates is significantly limited by the structural quality of these materials as a result of heteroepitaxy [1]. The advantages of using GaN substrate for homoepitaxy are low dislocation density (at least two orders lower than other substrates) and thermal expansion match, which significantly improved the performance and wafer bow, respectively. Furthermore, vertical devices could be grown on electrically conductive GaN substrates to reduce current crowding and self-heating effects of devices. Free-standing GaN substrates have been widely used in laser diodes (LDs) [2] and high-power light emitting diodes (LEDs) [3] owing to its low dislocation density and superior thermal electrical properties. Currently, free-standing GaN substrates can be successfully obtained by growing thick GaN film hetero-epitaxially on a foreign base substrate in hydride vapor phase epitaxy (HVPE), and subsequently separating from the original substrate using laser lift-off (LLO) [4], chemical lift-off [5], and self-separation [6]. However, the free-standing GaN substrates experience a serious issue of bowing, which makes the chemical mechanical polish (CMP) processes difficult and complicated. The bowing of free-standing GaN substrates has been suggested for nonhomogeneous distribution of threading dislocations and V_{Ga}–O_N complex defects in the growth direction, especially exit large amount at the N-polar face of *c*-plane free-standing GaN substrates [7,8]. Normally, a 2 in. free-standing GaN substrate with the bowing radius of 0.6–1.5 m may lead to 500–200 μm height difference between the center and edge of the free-standing GaN substrate, which may even be thicker than the GaN substrate itself [9,10]. This height difference of the free-standing GaN substrates owing to bowing may totally remove the GaN layer around the edge region, but may not polish the GaN layer around the center region during the CMP processes. In this study, we used ICP-etched N-polar face of the free-standing GaN substrate to modulate the bowing curvatures and directions, and then eventually obtained an extremely flat free-standing GaN substrate.

2. Experimental procedure

In the experiment, a 3-μm-thick GaN was initially grown on *c*-plane sapphire substrate using MOCVD as GaN template.

* Corresponding author at: Department of Electrophysics, National Chiao Tung University, 1001 University Road, Hsinchu 30010, Taiwan.
Tel.: +886 3 571 2121 56151; fax: +886 3 572 5230.
E-mail address: mapu.ep96g@g2.nctu.edu.tw (K.M. Chen).

0022-0248/$ - see front matter © 2010 Elsevier B.V. All rights reserved.
doi:10.1016/j.jcrysgro.2010.09.044

Subsequently, we used HVPE to grow 230-μm-thick GaN template by employing temperature ramping techniques developed in our earlier study [11]. During the growth of GaN in the HVPE reactor, NH_3 and GaCl generated from liquid gallium and HCl gas at 850 °C were used as the V and III group sources, respectively. The pressure was maintained at 700 Torr, and a mixture of H_2 and N_2 was applied as the carrier gas. Subsequently, the thick GaN film was separated from the sapphire substrate by LLO with a 355 nm Nd:YAG laser to make 230-μm-thick crack-free free-standing GaN substrate. Subsequently, the N-polar face of the free-standing GaN substrate was etched by ICP with increase in etching time from 7, 21, 35, 49, 63 to 77 min to examine the bowing phenomenon of the free-standing GaN substrate. In the series of ICP etching experiments, Cl_2 gas of 15 and Ar gas of 5 sccm were constantly transported into the chamber, while the coil power and platen power were fixed at 400 and 100 W, respectively.

The bowing radius of the free-standing GaN substrate was measured at the Ga-polar face using a spherometer. HRXRD was also applied at the Ga-polar face of the free-standing GaN substrate to measure the FWHM variation. The (0 0 2) diffraction peaks in X-ray ω-scan were identified using a Bede D1 system with the slit width of 0.5 mm. Surface morphology of the N-polar face of the free-standing GaN substrate after ICP etching was observed by scanning electronic microscope (SEM). Optical measurements of room-temperature photoluminescence (PL) were also performed at the Ga- and N-polar faces of the free-standing GaN substrate.

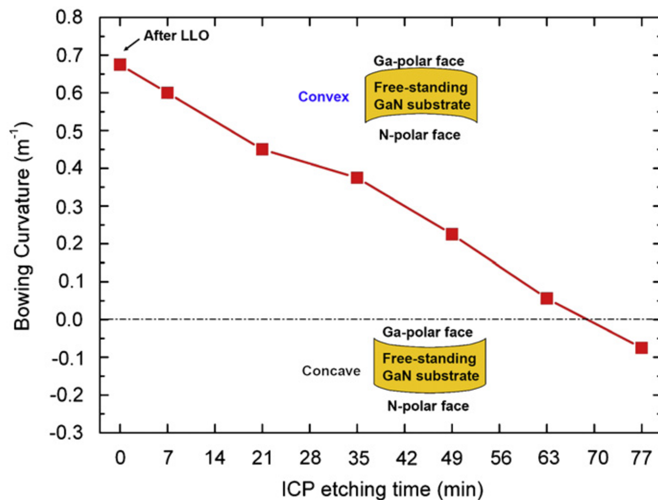

Fig. 1. Bowing directions and curvatures of the free-standing GaN substrate with increase in ICP etching time at the N-polar face.

3. Results and discussion

The variations in bowing curvatures and directions of the free-standing GaN substrate with increase in ICP etching time are summarized in Fig. 1. The bowing curvature has been defined as the inverse of the bowing radius obtained by a spherometer. When the thick GaN film was on the sapphire substrate before LLO, it bowed in convex direction with large bowing curvature of 3 m^{-1} owing to the thermal expansion mismatched between GaN and sapphire. After LLO, the bowing direction remained convex, but the bowing curvature clearly dropped. The bowing direction of the free-standing GaN substrate used in this experiment was different from other reports, including those from LLO [12], chemical lift-off [13], and self-separation [14]. The discussion on bowing direction of the free-standing GaN substrate produced by HVPE will be published elsewhere. We observed that the bowing curvature was significantly reduced to 0.67 m^{-1}, i.e., less bowing of the free-standing GaN substrate after LLO, which can be attributed to the relaxation of the thermal stress that originated from the sapphire substrate. After the application of ICP etching at N-polar face of the free-standing GaN substrate for 7 min, the bowing curvature further decreased to 0.59 m^{-1} and bowed in convex direction. With the further increase in the ICP etching time of up to 63 min, the bowing curvature almost linearly declined with the same convex bowing direction. The bowing curvature of the free-standing GaN substrate was only 0.056 m^{-1}, i.e., the bowing radius was 17.8 m when the ICP etching time reached 63 min. This value of bowing curvature was quite small and significantly improved when compared with the one before ICP etching. Moreover, with the further increase in the ICP etching time to 77 min, the bowing direction of the free-standing GaN substrate changed from convex to concave with a bowing curvature of 0.075 m^{-1}. It is interesting to note that the bowing direction of the free-standing GaN substrate can be varied from convex to concave. Thus, we can obtain free-standing GaN substrate without bowing at certain ICP etching time.

To confirm the variation in the bowing curvature of the free-standing GaN substrate with increase in ICP etching time, the HRXRD ω-scan in (0 0 2) reflection was applied at the Ga-polar face, as shown in Fig. 2(a). It could be observed that the FWHM decreased from 176.8 to 88.8 arcsec with increase in ICP etching time up to 63 min, similar to the trends of the variation in the bowing curvature. FWHM at the beginning of the ICP etching time

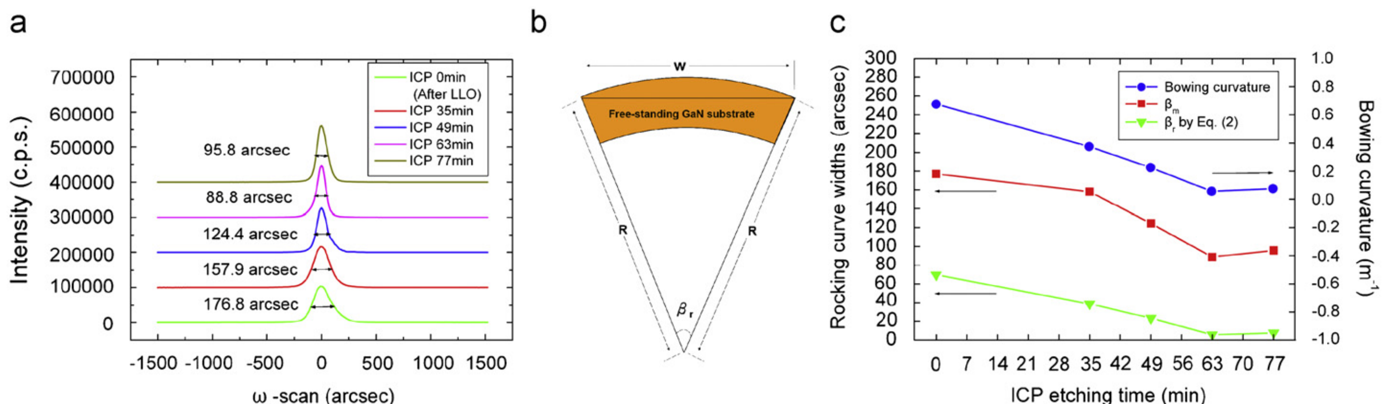

Fig. 2. (a) HRXRD ω-scan in (0 0 2) reflection at the Ga-polar face of the free-standing GaN substrate with increase in ICP etching time. (b) Schematic of geometry of the free-standing GaN substrate, where β_r is the broadening owing to the curvature of the crystal sample, R the bowing radius of free-standing GaN substrate, w the slit width in XRD measurements. (c) β_m values were measured from FWHM of (0 0 2) ω-scan and the β_r values were calculated from Eq. (2) with increase in ICP etching time.

for 7 and 21 min was not measured here. Furthermore, the FWHM slightly increased from 88.8 to 95.8 arcsec, along with the bowing curvature increasing from 0.056 to 0.075 m^{-1} as the ICP etching time increased from 63 to 77 min. The reports indicated that the measured FWHM of (0 0 2) symmetric XRD ω-scan was related to several components, as shown in Eq. (1) presented in Appendix A [15,16]. As there was no variation in the other components, except the bowing curvature under the ICP etching at the N-polar face, we concluded that the decrease in FWHM in XRD measurements was owing to the decrease in the bowing curvature. Furthermore, we intended to distinguish the effects of β_r from β_m. The geometry of free-standing GaN substrate is presented in Fig. 2(b). From the schematic, the formula of β_r could be derived from the trigonometric function, and can be given as

$$\cos(\beta_r) = (R^2 + R^2 - w^2)/(2RR) \quad (2)$$

The β_r values calculated from Eq. (2) are summarized in Table 1 and Fig. 2(c), which show similar trends and decrease in values with β_m and bowing curvature under increasing ICP etching time. This indicates that the influence of bowing curvature of the free-standing GaN substrate is obvious and serious, and the effects of the bowing curvature on the measured FWHM can simply be calculated using Eq. (2).

Fig. 3 shows the SEM images of the surface morphology at the N-polar face of the free-standing GaN substrate with different ICP etching time. From Fig. 3(a), it can be observed that the surface of N-polar face before ICP etching was flat with a little decomposition owing to LLO. After ICP etching of the N-polar face for 7 min, as shown in Fig. 3(b), the needle-like GaN appeared and the bowing curvature of the free-standing GaN substrate obviously decreased. With the increase in ICP dry etching time, the height and density of the needle-like GaN became longer and decreased separately, along with the continuous decrease in the bowing curvature of the free-standing GaN substrate, as shown in Fig. 3(c) and (d). The height and density of the needle-like GaN with increasing ICP etching time are shown in Fig. 4(a). It can be observed that the height of the needle-like GaN is linearly proportional to the ICP dry etching time, and the corresponding etching rate is around 2000 Å/min. Moreover, it can be noted that the needle-like GaN has high aspect ratio, because its inclined plane is unstable and easy to etch owing to larger dangling bonds (DBs). This results in vertical plane and high aspect ratio of needle-like GaN with increase in ICP etching time. Furthermore, we suggest that the decrease in the density of the needle-like GaN is related to the dislocation density. From Fig. 4(b), it can be noted that the dislocation density decreases with increase in distance from the N-polar face [17] owing to the fusion or annihilation reactions of dislocations. In our study, the density of needle-like GaN also decreased with increase in ICP etching depth from the N-polar face, and the slope was almost similar to the dislocation density. Yu et al. [18] reported that the dislocations tend to have weaker binding energy and could be easily dissociated by the ICP

Table 1
Summary of bowing radius and curvature, β_m calculated from measured FWHM of (0 0 2) ω-scan, and β_r from Eq. (2) with increase in ICP etching time.

ICP etching time (min)	Bowing radius (cm)	Bowing curvature (m^{-1})	β_m (arcsec)	β_r calculated from Eq. (2) (arcsec)
0	148.2	0.675	176.8	69.6
35	266.7	0.375	157.9	38.7
49	444.4	0.225	124.4	23.2
63	1777.8	0.056	88.8	5.8
77	1333.3	0.075	95.8	7.7

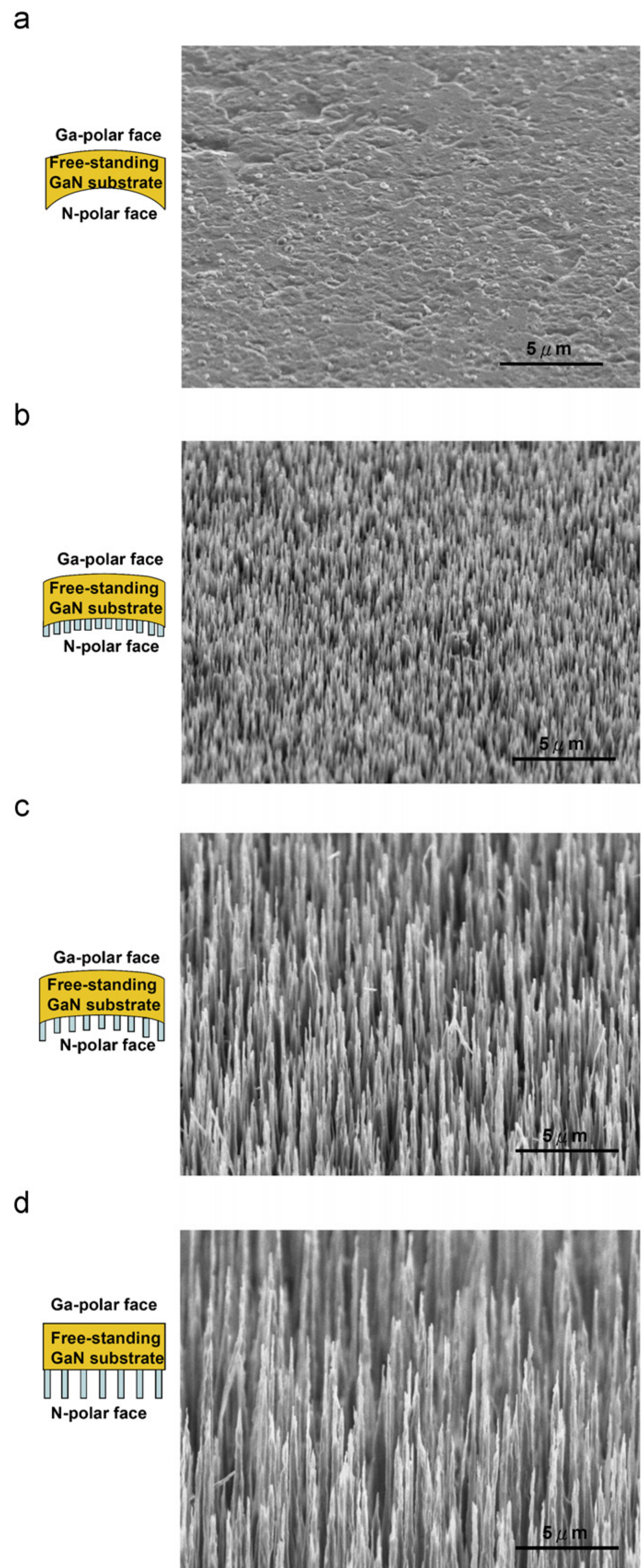

Fig. 3. SEM image at N-polar face of the free-standing GaN substrate under ICP etching time of (a) 0 min (after LLO), (b) 7 min, (c) 35 min, and (d) 77 min.

etching process, leaving behind rigid crystalline GaN region. Nonhomogeneous distribution of the threading dislocations in the growth direction causes bowing of the free-standing GaN

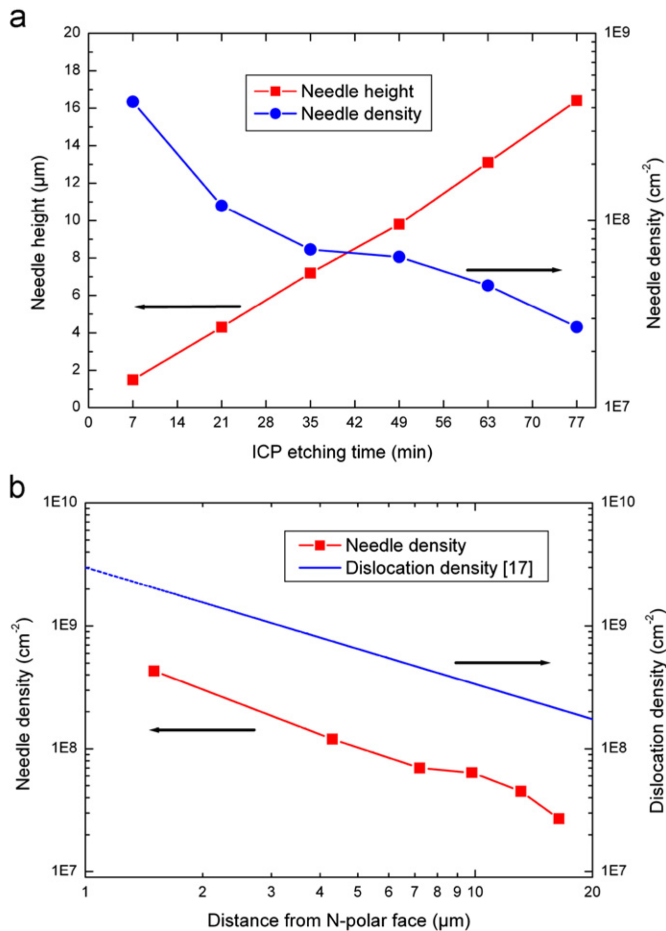

Fig. 4. (a) Height and density of the needle-like GaN substrate with increase in ICP etching time. (b) Density of dislocation [17] and needle-like GaN with increase in distance from the N-polar face.

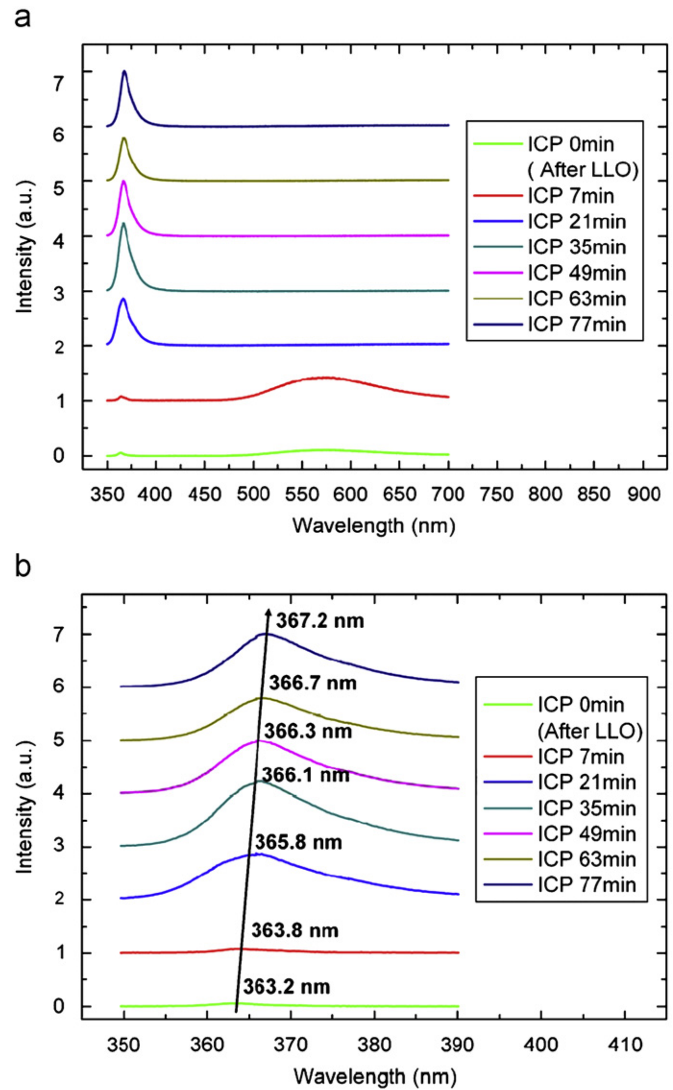

Fig. 5. (a) Room-temperature PL measurement at the N-polar face of the free-standing GaN substrate with increase in ICP etching time. (b) PL spectrum around NBE at the N-polar face of the free-standing GaN substrate with increase in ICP etching time.

substrates [7,8]. Therefore, decrease in the nonhomogeneous distribution of dislocations on removing the GaN layer from the N-polar face, which removes a large amount of dislocations, is the first reason for the improvement in the bowing of the free-standing GaN substrates by ICP etching. Moreover, the surface morphology of Ga-polar face remained flat before and after ICP etching since the ICP etching was applied at N-polar face.

PL measurements were carried out at the N-polar face of the free-standing GaN substrate with increase in ICP etching time, as shown in Fig. 5(a). The intensity of the near band edge (NBE) peak was very weak, but that of the yellow band (YL) peak was strong after LLO. After ICP etching for 7 min, the intensity of the NBE and YL remained the same. With the further increase in the ICP etching time from 21 to 77 min, the intensity of the NBE became stronger, but that of the YL disappeared. The intensity of the NBE was found to increase with the increase in the surface roughness, and change in the surface reflectivity and decrease in the defects were observed to act as nonradiative recombination centers [19]. Reshchikov and Morkoç reported that V_{Ga}–O_N complex defects increase the YL emission and decrease the density of V_{Ga}–O_N complex defects with increasing GaN thickness [20]. Thus, the stronger intensity of NBE with the ICP etching time exceeding 21 min could be attributed to the increase in roughness and decrease in nonradioactive defects, like threading dislocation as mentioned above. Furthermore, the intensity of YL disappeared as the ICP etching time exceeded 21 min, which could be owing to the decrease in the V_{Ga}–O_N complex defects. Thus, decrease in the nonhomogeneous distribution of the point defects as well as V_{Ga}–O_N complex defects on removing the GaN layer from N-polar face, which removes a large amount of point defects, is the second reason for the improvement in the bowing of the free-standing GaN substrates by ICP etching. It must be noted that the NBE and YL emissions after ICP etching for 7 min were similar to those after LLO. This is because the etching depth was about 1.5 μm. This thickness was still low in the MOCVD layer with large amount of threading dislocation and V_{Ga}–O_N complex defects, which resulted only in a slight decrease in the bowing curvature. Moreover, the PL measurements were also taken at Ga-polar face before and after ICP etching. The peak position, intensity, and FWHM of NBE showed no variation since the ICP etching was applied at N-polar face. Only the intensity of YL got a little large, which could be resulted from the impurity incorporated into Ga-polar face during the etching process.

Furthermore, it could be observed that the position of the NBE peak clearly red-shifted from 363.2 to 367.2 nm with increase in ICP etching time, as shown in Fig. 5(b). We suggest that the red-shift of the NBE peak can be attributed to the long and thin needle-like GaN that appeared at the N-polar face with increase in ICP etching time. This needle-like GaN released the compressive

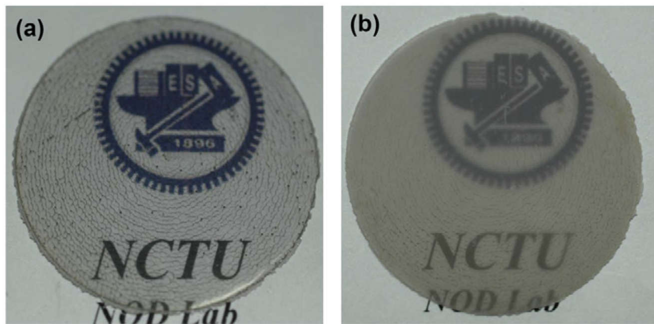

Fig. 6. Free-standing GaN substrate (a) before and (b) after ICP etching at the N-polar face.

strain at the N-polar face, which subsequently resulted in the change in the bowing direction from convex to concave. This is the third reason for the improvement in the bowing of the free-standing GaN substrates by ICP etching. It must be noted that the position of the NBE peak varied quite obviously from 363.8 to 365.8 nm as the ICP etching time increased from 7 to 21 min. This could be a result of the significant variation in the needle-like GaN density when ICP etching time increased from 7 to 21 min, as shown in Fig. 4(a).

4. Summary

In conclusion, the 230-μm-thick free-standing GaN substrate was obtained by HVPE and LLO. The N-polar face of the free-standing GaN substrate was etched by ICP with increase in etching time from 7 to 77 min to modulate the bowing curvatures and directions. The bowing curvature of the free-standing GaN substrate decreased almost linearly with increase in ICP etching time, which was only 0.056 m^{-1}, i.e., the bowing radius was 17.8 m when the ICP etching time reached 63 min (the bowing radius was 1.5 m at the beginning without ICP etching). Moreover, the bowing direction changed from convex to concave as the ICP etching time reached 77 min. Furthermore, the measured FWHM of (0 0 2) symmetric XRD ω-scan declined from 176.8 to 88.8 arcsec with increase in ICP etching time, confirming the decrease in the bowing of the free-standing GaN substrate, and the effects of the bowing curvature on the measured FWHM were also deduced. The correlation between bowing of free-standing GaN substrate and measured FWHM broaden due to bowing could be calculated by $\cos(\beta_r)=(R^2+R^2-w^2)/(2RR)$. SEM measurements revealed that the needle-like GaN appeared at the N-polar face after ICP etching. The height and density of the needle-like GaN became longer and decreased with increase in ICP etching time, respectively. This indicates that the decrease in the nonhomogeneous distribution of dislocations on removing the GaN layer from the N-polar face, which removes large amount of dislocations, is the first reason for the improvement in the bowing of the free-standing GaN substrates. PL measurements revealed that the intensity of the NBE became stronger, but that of the YL disappeared with increase in ICP etching time. This indicates that the decrease in the nonhomogeneous distribution of the point defects as well as V_{Ga}–O_N complex defects on removing the GaN layer from N-polar face, which removes large amount of point defects, is the second reason for the improvement in the bowing of the free-standing GaN substrates. Furthermore, the position of the NBE peak clearly red-shifted from 363.2 to 367.2 nm with increase in ICP etching time, showing that the released compressive strain at the N-polar face is the third reason for the improvement in the bowing of the free-standing GaN substrates. Finally, we were able to successfully obtain the flat and crack-free free-standing GaN substrate after ICP etching, as shown in Fig. 6(b).

Acknowledgements

This study is financially supported by the National Science Council of Taiwan through contract NSC 98-2221-E-009-026 and by the Minister of Education of Taiwan, which are deeply appreciated.

Appendix A

As the rocking curve is Gaussian in shape and by assuming Gaussian distributions of intensity for rocking curve components, the measured rocking curve FWHM, β_m is given by

$$\beta_m^2/2\pi=\beta_0^2+\beta_d^2+\beta_f^2+\beta_\alpha^2+\beta_\varepsilon^2+\beta_r^2 \tag{1}$$

where β_0 and β_d are the intrinsic rocking curve widths for the specimen and the analyzing crystals, respectively, β_f is the broadening owing to particle size, β_α the broadening caused by the angular rotation at dislocations, β_ε the broadening caused by the strain surrounding the dislocations, and β_r the broadening owing to the curvature of the crystal sample.

References

[1] T. Paskova, K.R. Evans, IEEE J. Sel. Topics Quant. Electron. 15 (2005) 1041.
[2] T. Obata, N. Kitajima, M. Ohta, H. Ichinokura, M. Kuramoto, Phys. Status Solidi (a) 205 (2008) 1096.
[3] K.J. Vampola, N.N. Fellows, H. Masui, S.E. Brinkley, M. Furukawa, R.B. Chung, H. Sato, J. Sonoda, H. Hirasawa, M. Iza, S.P. DenBaars, S. Nakamura, Phys. Status Solidi (a) 206 (2009) 200.
[4] E.A. Stach, M. Kelsch, E.C. Nelson, W.S. Wong, T. Sands, N.W. Cheung, Appl. Phys. Lett. 77 (2000) 1819.
[5] K. Motoki, T. Okahisa, N. Matsumoto, M. Matsushima, H. Kimura, H. Kasai, K. Takemoto, K. Uematsu, T. Hirano, M. Nakatama, S. Nakahata, M. Ueno, D. Hara, Y. Kumagai, A. Koukitu, H. Seki, Jpn. J. Appl. Phys. 40 (2001) L140.
[6] T. Yoshida, Y. Oshima, T. Eri, K. Ikeda, S. Yamamoto, K. Watanabe, M. Shibata, T. Mishima, J. Cryst. Growth 310 (2008) 5.
[7] D. Gogova, C. Hemmingsson, B. Monemar, E. Talik, M. Kruczek, F. Tuomisto, K. Saarinen, J. Phys. D: Appl. Phys. 38 (2005) 2332.
[8] T. Paskova, D. Hommel, P.P. Paskov, V. Darakchieva, B. Monemar, M. Bockowski, T. Suski, I. Grzegory, F. Tuomisto, K. Saarinen, N. Ashkenov, M. Schubert, Appl. Phys. Lett. 88 (2006) 141909.
[9] C. Hennig, E. Richter, M. Weyers, G. Trankle, J. Cryst. Growth 310 (2008) 911.
[10] D. Gogova, H. Larsson, A. Kasic, G.R. Yazdi, I. Ivanov, R. Yakimiva, B. Monemar, E. Aujol, E. Frayssinet, J.P. Faurie, B. Beaumont, P. Gibart, Jpn. J. Appl. Phys. 44 (2005) 1181.
[11] H.H. Huang, K.M. Chen, L.W. Tu, T.L. Chu, P.L. Wu, H.W. Yu, C.H. Chiang, W.I. Lee, Jpn. J. Appl. Phys. 47 (2008) 8394.
[12] B. Monemar, H. Larsson, C. Hemmingsson, I.G. Ivanov, D. Gogova, J. Cryst. Growth 281 (2005) 17.
[13] S.W. Lee, J.S. Ha, H.J. Lee, H.J. Lee, H. Goto, T. Hanada, T. Goto, K. Fujii, M.W. Cho, T. Yao, Appl. Phys. Lett. 94 (2009) 082105.
[14] Ch. Hennig, E. Richter, U. Zeimer, M. Weyers, G. Tränkle, Phys. Status Solidi (c) 3 (2006) 1466.
[15] M.J. Hordon, B.L. Averbach, Acta Metall 9 (1961) 237.
[16] J. Chaudhuri, M.H. Ng, D.D. Koleske, A.E. Wickenden, R.L. Henry, Mater. Sci. Eng. B 64 (1999) 99.
[17] S.K. Mathis, A.E. Romanov, L.F. Chen, G.E. Beltz, W. Pompe, J.S. Speck, Phys. Status Solidi (a) 179 (2000) 125.
[18] C.C. Yu, C.F. Chu, J.Y. Tsai, H.W. Huang, T.H. Hsueh, C.F. Lin, S.C. Wang, Jpn. J. Appl. Phys. 41 (2002) L910.
[19] D. Basak, Q. Fareed, K. Nishino, S. Sakai, J. Vac. Sci. Technol. B 18 (2000) 2491.
[20] M.A. Reshchikov, H. Morkoç, J. Appl. Phys. 97 (2005) 061301.